Table S1. IPA analysis network list

ID	Molecules in Network	Score	Focus Molecules	Top Diseases and Functions
1	ARHGEF1,ATP5F1B,BRD4,CXCR4,CYTIP,FBL,MAP3K8,MDH1,NFKBIZ,RHOH,RPL10A,RPL15,RPL22,RPL23A,RPL3,RPL30,RPL31,RPL38,RPL4,RPL5,RPL6,RPL9,RPLP0,RPS13,RPS16,RPS2,RPS23,RPS3,RPS4X,RPSA,TALDO1,TCR,TLE3,TLR7/8,UBA52	36	33	[Cancer, Protein Synthesis, RNA Damage and Repair]
2	Actin,AGER,ANXA1,BIRC5,CCNB1,CCNB2,CD55,CDC20,CDCA2,CDCA8,CDK1,CENPA,CENPE,CENPF,CLIP1,Cyclin A,DARS,DGKA,FLNA,FOXM1,GTSE1,IKBKB, INPP5D, INPPL1, KIF11,KIF20A,MAL,OGT,P38 MAPK,PLEC,PLK1,PRC1,RALA,TJP2,UBE2C	34	32	[Cell Cycle, Cellular Assembly and Organization, DNA Replication, Recombination, and Repair]
3	B2M,CD69,CYP19,ERK1/2,FGFR1,GIT1,HLA-C,HLA-F,HSF4,IL12 (family),IL23,JAK3, KIF2C, KMT2C,MAP3K10,MAP3K11,MAP3K5,MAP4,MC1R,MYO18A,NCOR1,NCOR2,PHB,PHB2,POLR2A,PSMB6, PSMB8,PSMB9,RAP1A,SCRIB,TAP1,TAPBP,TNFRSF25,TNFSF15,TXN	32	31	[Antigen Presentation, Hematological System Development and Function, Protein Synthesis]
4	26s Proteasome, Akt, AURKB,CARD11,CCR4,CDKN2C, CNTRL,CYSLTR1,DNMT1, DNMT3B,DPP4,ERO1A,FES,FOXP3,GAB2,Hsp70,IL7R,MAF,MDM4,Mek,NISCH,NOTCH1,PCNT,RACK1,Rb, SH3PXD2A,SHCBP1,SLC35F3,SMARCA2,SMOOTH MUSCLE ACTIN, STAT5a/b,STK11,UXT,VPS13A,ZNF335	26	28	[Cancer, Lymphoid Tissue Structure and Development, Tissue Morphology]
5	ACADVL,ADAM19,APOBEC3G,BCL6,BCL7B,C1QBP,CSF1,EEF1A1,ERN1,EVL,Focal adhesion kinase,GBP1,GBP5,GIMAP4,IFITM1,IFN Beta,Ige,IgG,IL12 (complex),IL13, IL18BP, Interferon alpha, LDL, MYL12B, NLRC5, NLRP1,PARP10, PPM1K,SRC (family), STAT1,STAT2,TRIM22,TYK2,UBA7,UBE2L6	25	27	[Cellular Function and Maintenance, Immunological Disease, Infectious Diseases]
6	AGAP2-AS1,BCL11B,BCL2,caspase,CG,COL18A1,CREBBP,Cyclin E,DLG4,ECE1, EIF4G1,EOMES,EP300,ERK,GSTP1,H6PD,HIF1A,Histone h3,ILK,Jnk,KDM4B, MKI67, NRP2,PARK7,PARP,Pkc(s),PTGIS,RGS10,RRM2,SH3BP2,Smad2/3,STK10,TMPO,Vegf,VHL	22	25	[Cell Morphology, Hematological Disease, Respiratory Disease]
7	AGAP2,ARID1A,BCR(complex),CD3,CD4,CD5,EP400,FANCA,Hsp90,Igm,KDM6B,MAP3K14,MAVS,MTORC1,NCL,NFkB (complex),p70 S6k,PAG1,PI3K (complex),PI3K (family), PI3K p85, PLCG1,PRKAA,PRR14,RAB11A,RPS6,SAMSN1, SMARCA4, SMARCC2, SPN, SRCAP, TNFRSF8, UNC13D,WAS,ZAP70	20	24	[Hematological System Development and Function, Hematopoiesis, Tissue Morphology]
8	ACTN1,ACTR2,ADCY7,ADCY9,ARHGAP1,ARL6IP5,BETA TUBULIN,CAMK2G,CDK16, CREBZF,CSF2RB,CSNK1A1,FSH,FYB1,GBP1,GRK5,HSD11B1,ITGB5,Lh,MAP3K5,MEF2D,MMP25,MSMO1, PLPP1,PTP4A1,SMARCD1,STK17A,TAGLN,TLK1,TLN1,TMBIM6,TPM2,TRIB1,TYRO3,YTHDF2	16	21	[Cellular Assembly and Organization, Cellular Compromise, Cellular Development]
9	AKNA,AREG,CCNA2,CD3D,CDC25A,CDCA3,CDK1,CTLA4,DMBT1,E2F1,E2F3,E2F4,H19,HDAC1,KDM5B, LTBP3,MALAT1,MAPK8IP3,MIA,MT1X,MYBL2,NCAPG2,PDCD1,RB1,RBL1,RBL2,RRM2,SMARCA2,SMG6,SOX9,TM9SF2,TOP2A,TPX2,TYMS,ZBTB7A	12	18	[Cell Cycle, Connective Tissue Development and Function, Embryonic Development]
10	ADAM8,APP,BIK,BIRC5,CCL18,COLQ,COX4I1,CYBA,CYBB,EBI3,EPM2AIP1,GIPR,GLUL,HAS1,HIVEP1,HSPA8,IFNAR2,IL15RA,IL17RB,IL36RN,KLF6,MAFF,MYO9B,NOS2,PSME2,S100A6,SCO2,SLAMF7,SMPD2, TNF,TNFAIP2,TNFSF15,TREM1,TSPYL2,YBX1	11	17	[Cell Death and Survival, Lipid Metabolism, Organismal Injury and Abnormalities]
11	Akt,CCN2,CCND1,CCT2,CCT4,CCT6A,CCT7,CDK5RAP2,CELF1,CLOCK,COL18A1,COPG1,CTNNB1,CXCL12,EGFR,ERK,ESR1,EZH2,FANCI,HIF1A,Jnk,MCOLN3,MYBBP1A,NFkB (complex),NUMA1,PIK3CA,SEC23A,STAT3,SUGP2,TGFBR2,UBE2N,UHMK1,WWC3,YAP1,ZEB1	11	17	[Cancer, Cell Death and Survival, Organismal Injury and Abnormalities]
12	ADAM12,ATP2A3,CD4,CD48,CDC42BPG,CYP17A1,FLOT1,GRK2,HAVCR2,HDAC7,ICOS,IFNG,INF2,JUNB, LCK,Lfa-1,MYL12A,NCR2,NFIC,NONO,NR4A1,PDE4A,PDE8A, PPP1R9B, PPP2CA,PTPN6,RGS18,SLAMF6,SP1,SPN,TCF7L2,TCIRG1,TYK2,YLPM1,ZAP70	11	17	[Cell Death and Survival, Cellular Compromise, Immunological Disease]
13	ANXA11,ATG10,BAX,BRCA1,CASP2,CDK2,CDKN1A,CFLAR,CHD3,CKS2,CTNNB1,ELAVL1,ESR1,ESR2,HOXC6,HSF1,HSP90AB1,KIF23,KMT2A,KMT2D,KRT10,KRT6A,MBOAT7,MDM2,NCOR1,NXF1,PCNX2,POLR2A,PSMB4,RPL13,S100A8,SAFB,SPTAN1,TP63,UBB	11	17	[Cancer, Hematological Disease, Immunological Disease]
14	ACIN1,BCOR,BTG1,CAMP,CARM1,CASP3,Caveolin,CD3,DMTN,F2,FLNA,FTL,FYB1,IQGAP2,ITGB1,ITPKB,ITPR3,KCNA3,LCP2,LTB4R,miR-515-3p (and other miRNAs w/seed AGUGCCU),Mlc,MPRIP,OBSCN,PDLIM1,PPP1R12A,PRMT1,PTK2B,RHOA,RIPK1,Rock,STIM1,TC2N,TRPC1,ZYX	11	17	[Cell Morphology, Cell-To-Cell Signaling and Interaction, Cellular Movement]
15	BAP1,BIRC2,CASP8,CASP9,CDKN1B,CEBPB,DAP3,DAPK1,E2F1,EP300,FADD,FASLG,FOXK1,FOXK2,GADD45A,HCFC1,IGF1R,IL11RA,INPP4A,mir-17,NAP1L1,POLH,PTP4A3, RABL6,RPL26,SRSF3,STMN1,TNFRSF10A,TNFRSF10B,TNK2,TP53,TP53COR1,TP53INP1,TP73,TYMSOS	9	15	[Cell Death and Survival, Embryonic Development, Organismal Injury and Abnormalities]
16	ATM,CCNL2,ESPL1,GADD45G,GATA4,GATA6,GATAD2A,GSC,H2AFX,HNRNPH1,HNRNPUL1,HOPX,HOXB1,HOXB3,MAPK8,MDC1,MEIS1,MRE11,NANOG,NBN,NME2,NPTX1,NR6A1,NUSAP1,PHACTR2,POU5F1,PPP2R5D,PRRC2C,RAD50,RBBP8,REST,SOX17,TAOK2,TERT,TNFRSF11A	9	15	[Cell Cycle, DNA Replication, Recombination, and Repair, Embryonic Development]
17	AKT1,AR,AREG,CCNA2,DICER1,EDN1,EGF,EGFR,EIF3E,EPAS1,ERG,ERK,ETS1,FLNB,FOXM1,GAK,HJURP,HRAS,Hsp90,IQGAP3,KDR,MET,NOS3,NPHP1,NPHP4,PTPRJ,RASSF1,RSU1,SNAI1,SPTBN5,TP53,UTRN,VEGFA,ZDHHC21	8	14	[Cellular Movement, Embryonic Development, Organismal Development]
18	ACACB,ACTR3,ADIPOQ,ANG,APOA1,ARHGEF4,C1q,CABIN1,CCL2,CD163,DNM2,FLT3LG,HBE1,HBZ,HDL,HGF,HMGB1,IGHE,IL17RA,IL25,IL4,IL6,IQGAP1,JAG2,MYH9,RAC2,RPS19,RPS5,S100A9,SEMA4D,SLAMF7,SPN,STK11,TAL1,TXLNA	8	14	[Cellular Development, Cellular Growth and Proliferation, Hematological System Development and Function]
19	ACAN,ALOX5,Alp,ANPEP,ASH2L,BMP2,CCNE1,CCT5,CDKN1A,CDKN2B,CUL4A,Cyclin E,DDB1,FOXM1,GSDMB,HEY1,JAG1,KLF5,LIG1,MRTFA,MT-TY,MYC,PDLIM7,PRDM16, RB1CC1,RBL1,RPL11,RPS14,SKI,SMARCB1,SP7,TAF1C,TCP1,TGFB1,XYLT1	8	14	[Cell Cycle, Cellular Development, Cellular Growth and Proliferation]
20	ATF3,BDNF,CASP1,CXCL8,CXCR2,DHCR24,Eotaxin,FCER1G,GATAD2B,Hdac,HMGB1,IKBKE,IL13,IL1A,IL1R2,IL25,IL36G,JAG1,JUP,MAN2B2,miR-155-5p (miRNAs w/seed UAAUGCU),MYO1E,NFKBIZ,PDCD1,PIEZO1,PREX1,S100A9,SERPINB4,SPINT2,SPN,TGFBR2,TMSB10/TMSB4X,TPT1,ZC3H12A,ZMIZ1	8	14	[Cellular Movement, Hematological System Development and Function, Immune Cell Trafficking]
21	ACTB,ARHGAP33,ARL2,ARPC2,CDH1,CDKN2B,CELF1,DAB2IP,DNMT1,ETV5,EZH2,F Actin,HDAC1,HNRNPU,HOXA11-AS,HULC,IL2RB,JARID2,KLF2,LSP1,MECP2,mir-8,MYOD1, NKD2,NSD2,PIP5K1C,RBBP6,SPRY4-IT1,SPTBN1,SUZ12,TMOD3, UCA1, ZEB1,ZEB2, ZFAS1	8	14	[Cellular Development, Cellular Growth and Proliferation, Infectious Diseases]
22	ACTA2,AGO1,AGO2,AMT,ANKRD12,BAX,CCL2,CDC25A,CHD7,CPSF1,CXCL12,CXCR4,F13A1,IGF1,ILF3, INHBA,let-7,MAFB,mir-199,mir-21,mir-342,mir-8,MYD88,NFKB1,PIDD1, POGZ, PTBP2,PTGIR,RPLP1,RPLP2,SATB1,SERPINB2,SNRPC,SORBS3,TNRC6B	8	14	[Inflammatory Disease, Organismal Injury and Abnormalities, Respiratory Disease]
23	ADAM17,AKT1,ANXA9,ATF1,CALCA,Calmodulin,CD163,CFL1,Cpla2,CSF2,DNMT1,FCER1G,GAS5,Hdac,ICOS,IFNB1,IKBKE,IL1B,IL24,LTB,LUC7L3,MMP12,MRC1,NACA,NEAT1,PDGF BB,PPA1,PTGS2,RALB,RREB1,S1PR1,SH3BP2,SSH1,TGFA,TLR5	7	13	[Gastrointestinal Disease, Inflammatory Disease, Inflammatory Response]
24	ACTN4,AKAP13,ANGPTL4,APH1A,APOA1,BCL2,CD163,CD46,CLK1,CTNNB1,CXCR4,DCN,DDX17,DERL1,DROSHA,hemoglobin,HMOX1,IDO1,Ifn gamma,Ige,IL10,IL12B,LEP,MIAT,mir-150,NFKBIA,NOS2,NR3C1,SELPLG,SERPINA1,STAT5a/b,TCF,TSC22D3,TSSK3,ZMAT3	6	12	[Cancer, Cellular Development, Cellular Growth and Proliferation]
25	Akt,ARAP1,ASPM,ATF2,CCL20,CPT1A,CXCL10,DEPDC1,DLGAP5,DRAP1,EIF2AK3,ERK,FOXO1,GCG,HNF1A,IGF1,IGF2BP2,IGFBP1,IL6,INS,IRS1,MAPK1,MAPK3,NCAPG,PGR,PRL,RAN,RPL7A,SNX17,TARS,TRPC1,TWIST1,UQCRC2,Vegf,ZCCHC2	6	12	[Endocrine System Disorders, Hematological Disease, Metabolic Disease]

Supplementary Methods

Generation of "cultured T_{CM}" $CD4^+$ primary T-cells

Latency model cells were generated as previously described (*1*). $5x10^6$ naïve $CD4^+$ T cells from HIV^- or HIV^+ were isolated by magnetic negative selection (StemCell Technologies), then cultured at 10^6 cells/mL in 96-well plates using R-10 media (RPMI-1640 media supplemented with 10% FBS, 2mM L-glutamine, 100 units/ml Penicillin and 100µg/ml Streptomycin) supplemented with 12.5uL/mL of dynabeads human T-activator CD3/CD28 (Invitrogen), 2µg/mL anti-human IL-12 (PeproTech), 1µg/mL anti-human IL-4 (PeproTech), and 10ng/mL of TGF-β1. After 3 days, dynabeads were removed by magnetic selection and cells were washed, followed by culture in R-10 media supplemented with 30 IU/mL of IL-2 (R-10-30). Media was changed on days 4 and 5 with fresh R-10-30 media.

Infection of "cultured T_{CM}" cells to generate latency model

On day 7 of the above "cultured T_{CM}" generation protocol, 1/5th of the cells were infected with HIV_{NL4-3} at a MOI of 0.6 by spinoculating at 2900 x g for 2 hours, at 37°C. Cells were then resuspended in R-10-30 with the other 3/5th of the cells and placed back in the incubator, while the remaining 1/5th were set aside as an uninfected control. On day 10, cells were recounted, washed and resuspended in R-10-30 at 10^6 cells/mL and plated in 96-well round bottom plates to crowd infection. On day 13, cells were washed and resuspended at 10^6 cells/mL, and then transferred to culture flasks in R-10-30 supplemented with 1µM Raltegravir and 0.5µM Nelfinavir at 10^6 cells/mL. On day 17, CD4 positive cells were isolated by magnetic positive selection following the manufacturer's instructions (Life Technologies), and then used in the various assays. A small portion of the cells were reactivated with CD3/CD28 dynabeads and stained for intracellular Gag, to determine infection percentages and ensure quality controls.

"cultured T_{CM}" primary cell latency model "spiked" HIV Eradication (HIVE) Assays

HIVE assays were set up as previously described (2). Briefly, >20 x 10^6 $CD4^+$ T cells were pulsed with bryostatin or anti-CD3/CD28 antibodies, then washed and co-cultured with/ without ABT-199 in XVIVO-15 media (Lonza) supplemented with 1µM Tenofovir Disoproxil Fumarate, 1µM nevirapine, 1µM emtricitabine, 10µM T-20, 10U/ml human DNAse I (ProSpec), and 0.1nM IL-7 (HIVE media). Primary latency model cells were spiked into newly isolated, autologous resting $CD4^+$ T-cells to achieve a frequency of ~1,000 – 10,000 copies of HIV DNA per million CD4+ T-cells. Following a 3-4 days co-culture, $CD4^+$ T cells were isolated and rested for 24 hours in R10-50 media at 37ºC to allow for an ARV

washout period. Aliquots of pre- and post- CD4 enrichment samples were collected and stained for viability and memory phenotype/activation status with antibodies against CD3, CD4, CD8, CD45RA, CD69, and CCR7, then analyzed by flow cytometry. Following the overnight culture, a small aliquot of cells was mixed with CountBrightTM absolute counting beads and viability dye (Invitrogen Technologies) to obtain a count of total, live CD4+ T-cells by flow cytometry. This viable cell count was used to determine cell numbers for ddPCR and QVOA plating strategies.

HIV-specific T-cell (HST) generation

HIV-specific T-cell (HST) lines were generated as previously described (*3, 4*). Briefly, dendritic cells (DCs) were isolated by plastic adherence from PBMCs, and incubated for 6 days with IL-4 (1000 U/mL) and granulocyte macrophage colony stimulating factor (GM-CSF) (800 U/mL). On day 7, DCs were matured with IL-4, GM-CSF, LPS (30 ng/mL; R&D), IL-6 (100 ng/mL; R&D), TNF-a (10 ng/mL; R&D), IL- 1b (10 ng/mL; R&D), and Prostaglandin E2 (1 mg/mL; Sigma-Aldrich). DCs were harvested 24 – 48 hours after maturation, and matured DCs were pulsed with Gag, Pol, and Nef pepmixes (0.2 mg/mL) (JPT, Berlin). Non-adherent cells (T-cells) were thawed and stimulated with DCs at a ratio of 1:10 (10^5:10^6 cells/well; DC:CTL). For priming/Stimulation 1, IL-7 (10 ng/mL), IL-12 (10 ng/mL), and IL-15 (5 ng/mL) (all R&D Systems) were used. T-cells were re-stimulated after 7-10 days for Stimulation 2 with autologous, irradiated (3,000 rad), pepmix-pulsed PHA blasts, at a stimulator-to-responder ratio of 1:4 and maintained with IL-15 (5 ng/mL). To generate phytohemagglutinin blasts (PHAb), PBMCs were stimulated with PHA-P (5 µg/ mL; Sigma-Aldrich) in the presence of IL-2. For Stimulation 3, (7 days post-Stim 2), HIV-specific T-cells were restimulated with PHAb as above, in the presence of IL-2 (50 U/ mL) and were fed or split if they became confluent in between stimulations with IL-2.

T-cell cloning and maintenance

$CD8^+$ T-cell responses in subjects were mapped by IFN- γ ELISPOT, using 270 previously defined HIV optimal $CD8^+$ epitopes restricted by common HLA alleles. For each response, PBMCs from HIV+ donors were plated at $1x10^7$ cells/well in a 24-well plate and stimulated with 10 µg/ml of peptide for 3 hours. T-cells producing IFN- γ in response stimulation were enriched using the IFN- γ secretion detection and enrichment kit (Miltenyi Bioetc), following the manufacturer's instructions. The isolated cells were plated at a series of dilutions in 96-well plates with feeder medium (R-10 with $1x10^6$ cells/ml 5,000 rad irradiated PBMC + 50 U/ml IL-2 + 0.1 µg/ml each of anti-CD3 (OKT3, Biolegend), anti-CD28 (CD28.2, ebioscience). After 4 weeks, colonies were selected from the lowest dilution plate with positive wells (<1/5 of

wells positive) and screened for responsiveness to peptide by CD107a staining on flow cytometry following stimulation with cognate peptide. Positive clones were expanded every 2-3 weeks with fresh feeder medium, and clone specificities were confirmed by degranulation assay (CD107a flow cytometry) prior to each expansion, and the day prior to use in any assay.

Fig. S1. Ingenuity pathway analysis comparing CD4^{+} T-cells that co-cultured with activated CTL compared to non-activated CTL. Shown are the top 30 significantly enriched pathways comparing 'real bystanders' to 'mock bystanders' (left panel), or 'real survivors' vs 'mock survivors' (right panel). Differential expression genes (DEGs) were

determined with a cut-off of FDR <0.05 and FoldChange >1.5 (log2FoldChange >0.585). Pathway scoring method is using B-H Multiple Correction p-value, and threshold is set at a -log(B-H p-value) >1.3. Orange bars represent positive z-scores, blue bars - negative z-score and grey bars - no activity pattern. The results indicate that differences between 'real bystanders' and 'mock bystanders' primarily reflect cytokine and interferon signaling as a result of the former being co-cultured with peptide-stimulated CTL. The differences between 'real survivors' and 'mock bystanders' is a hybrid between the differences between 'real bystanders' vs 'mock bystanders' and 'real bystanders' vs 'real survivors'. These relationships are also depicted in the principal component analysis plot shown in **Fig. 1B**.

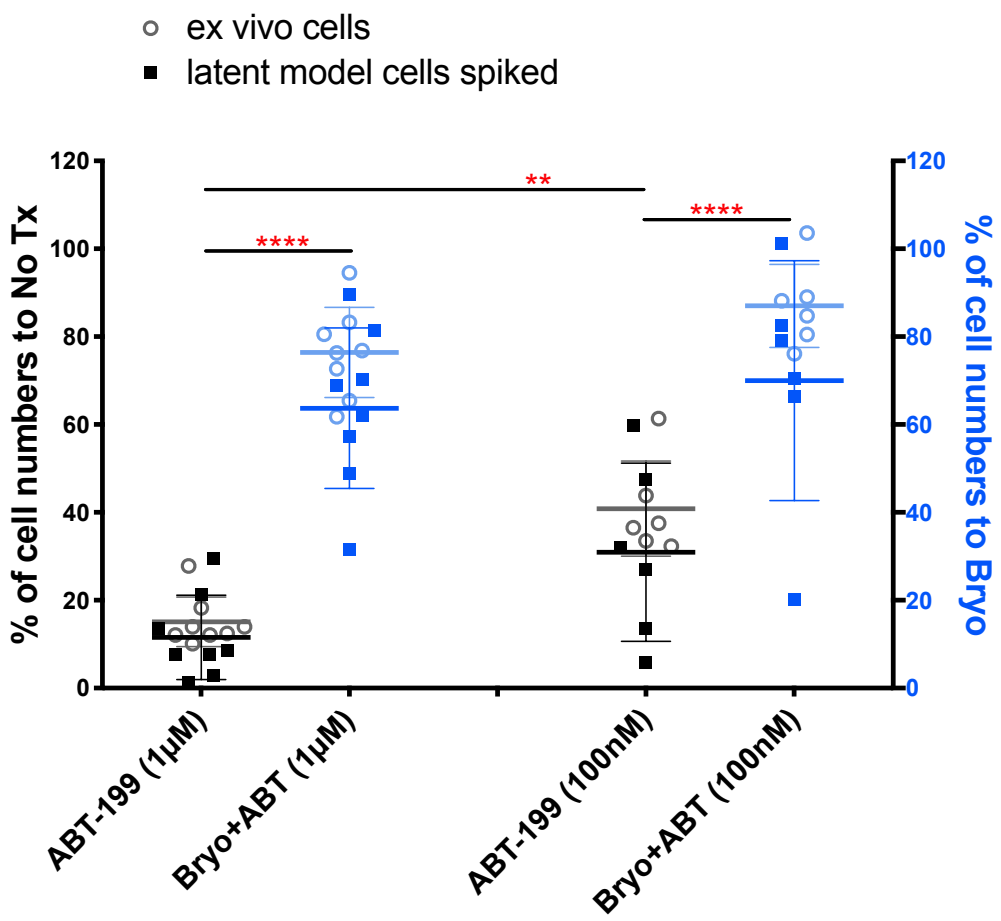

Fig. S2. Cell Toxicity of BCL-2 Antagonist on Primary Cell Latency Model and Patient-derived *Ex Vivo* Cells. Percentage of cell numbers in each ABT-199 concentration treatment compared to No Tx (black), or combination of Bryostatin-1+ABT-199 treatment compared to Bryostatin-1 (blue). Shown is the cell count percentage mean ± SD from separate HIVEs. Statistical significance determined by One-way ANOVA. * $p<0.05$, ** $p<0.01$, **** $p<0.0001$.

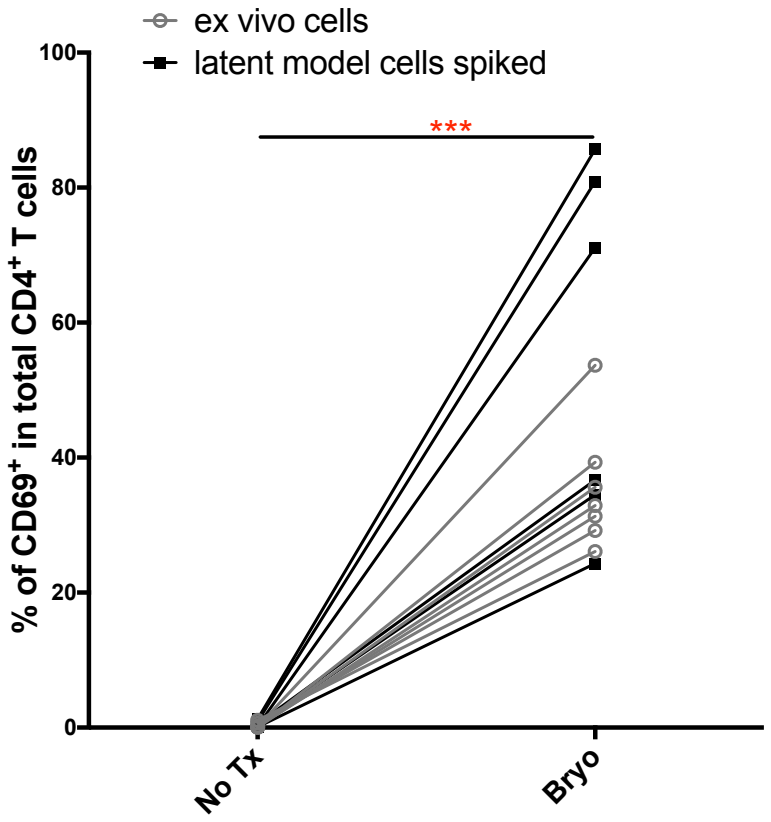

Fig. S3. Bryostatin-1 Potently Activated CD4$^+$ T-cells in HIVE Assays. CD69 expression was measured on viable CD4+ T-cells sampled at the termination of HIVE assays, showing no treatment (No Tx - range: 0.04%-1.29%, mean: 0.44%) vs Brystatin-1 treated (Bryo - range: 26.1%-85.7%, mean: 44.3%). Statistical significance determined by Wilcoxon matched-pairs signed rank test.

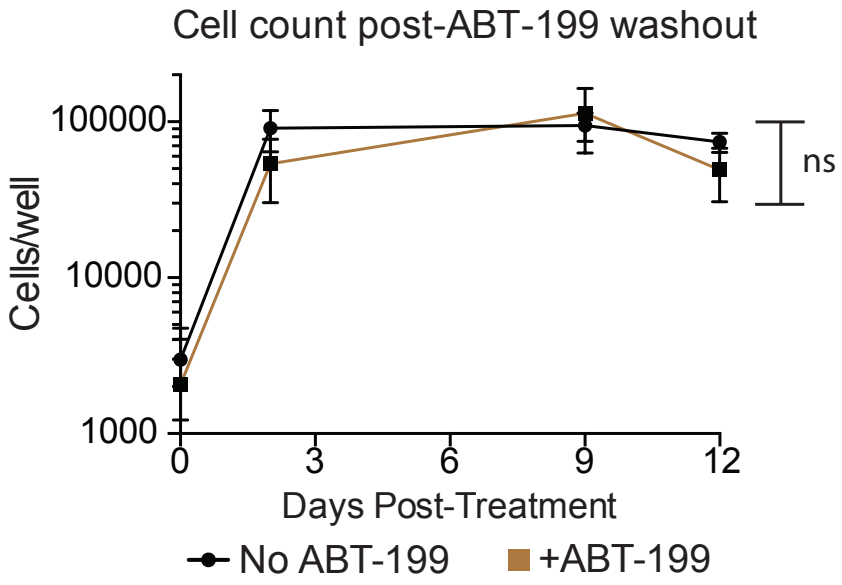

Fig. S4. ABT-199 Does Not Continue to Affect CD4$^+$ T-cell Viability after Plating in QVOAs (post-HIVE assays). We observed that ABT-199 treatment resulted in appreciable loss in cell viability over the course of the HIVE assay co-cultures (**Fig. S2**). In order to prevent this from affecting QVOA quantifications, we washed cells at the conclusion of HIVE assays, cultured overnight to allow for any in progress cell death to proceed, then counted viable CD4$^+$ T-cells by flow cytometry and used these numbers to calculate infectious units per million (IUPM). A concern remained that ABT-199 may continue to impact the viability of CD4$^+$ T-cells after wash-out/plating and that this could affect QVOA results. The data shown here rules out this effect. Shown are counts of viability of CD4$^+$ T cells from QVOA wells as determined by flow cytometry (in relation to counting beads) over 12 days of culture. No significant differences in cell viability were seen between CD4$^+$ T cells from "No ABT-199" vs. "+ABT-199" conditions. The results confirm that the effects of ABT-199 on viability do not appreciably persist beyond an overnight wash-out period, and thus support the reliability of the QVOA quantifications on these samples. Note also that if lingering effects of ABT-199 on overall cell viability were responsible for decreasing QVOA measurements then we would have expected to see that the various ABT-199 treatment conditions performed in the absence of CTL to also drive apparent reductions in IUPM (QVOA), ex. in **Figs. 5&7**, which was not observed.

The BCL-2 Antagonist ABT-199 Drove Reductions in Total HIV DNA and Infectious Reservoirs in a Primary Cell Latency Model

We tested the BCL-2 antagonist ABT-199 in a well-characterized primary cell model of HIV latency (*1, 5*) by spiking into autologous $CD4^+$ T-cells (**Fig. S5A**). The latent model cells were generated from either an HIV-negative donor (**Fig. S5B**) or a HIV-positive donor (**Fig. S5C**), and we observed significant reductions in total HIV DNA as measured by *gag* primer/probe sets following treatment with ABT-199 (at both concentrations, 1μM and 100nM) alone or in combination with latency reversal agent bryostatin-1 (**Fig. S5B-C, left lanes**). Combination treatments with bryostatin-1 and ABT-199 significantly reduced HIV DNA relative to ABT-199 alone, more strictly in HIV-negative donor generated model cells (**Fig. S5B-C**). Similar with *ex vivo* $CD4^+$-T cell HIVEs, we also observed overall loss in viability when treated with ABT-199 and combination with bryostatin-1 mitigated the toxicity, where we observed a 130-fold reduction in IUPM in the bryostatin-1 + 1μM ABT-199 condition ($p<0.0001$), and a 21-fold reduction in IUPM in the bryostatin-1 + 100nM ABT-199 condition ($p<0.0001$, **Fig. S5B**) for the HIV-negative donor latency model; a 99-fold reduction in IUPM following treatment with bryostatin-1 + ABT-199 (1μM) ($p<0.0001$) and a 39-fold reduction in bryostatin-1 + ABT-199 conditions (100nM) ($p<0.0001$, **Fig. S5C**) for the HIV-positive donor latency model.

We tested this BCL-2 antagonist against latency model cells generated from 4 HIV-negative and 4 HIV-positive donors. Treatment with 1μM or 100nM ABT-199 resulted in significant decreases in HIV DNA when combined with bryostatin-1 or used alone ($p=0.02$ for both conditions, **Fig. S5D-E left**). A significant reduction in IUPM was also observed for the combination with bryostatin-1 when ABT-199 was used at 1μM ($p<0.01$, **Fig. S5D right**). We were limited in our ability to assess reductions in IUPM with this high concentration of ABT-199 alone due to insufficient cell numbers for QVOA in some experiments as a result of toxicity (**Fig. S5D right**). Together, these results demonstrate that BCL-2 antagonist ABT-199, used alone or in combination with bryostatin-1, are sufficient to drive reductions in a primary cell model of HIV latency.

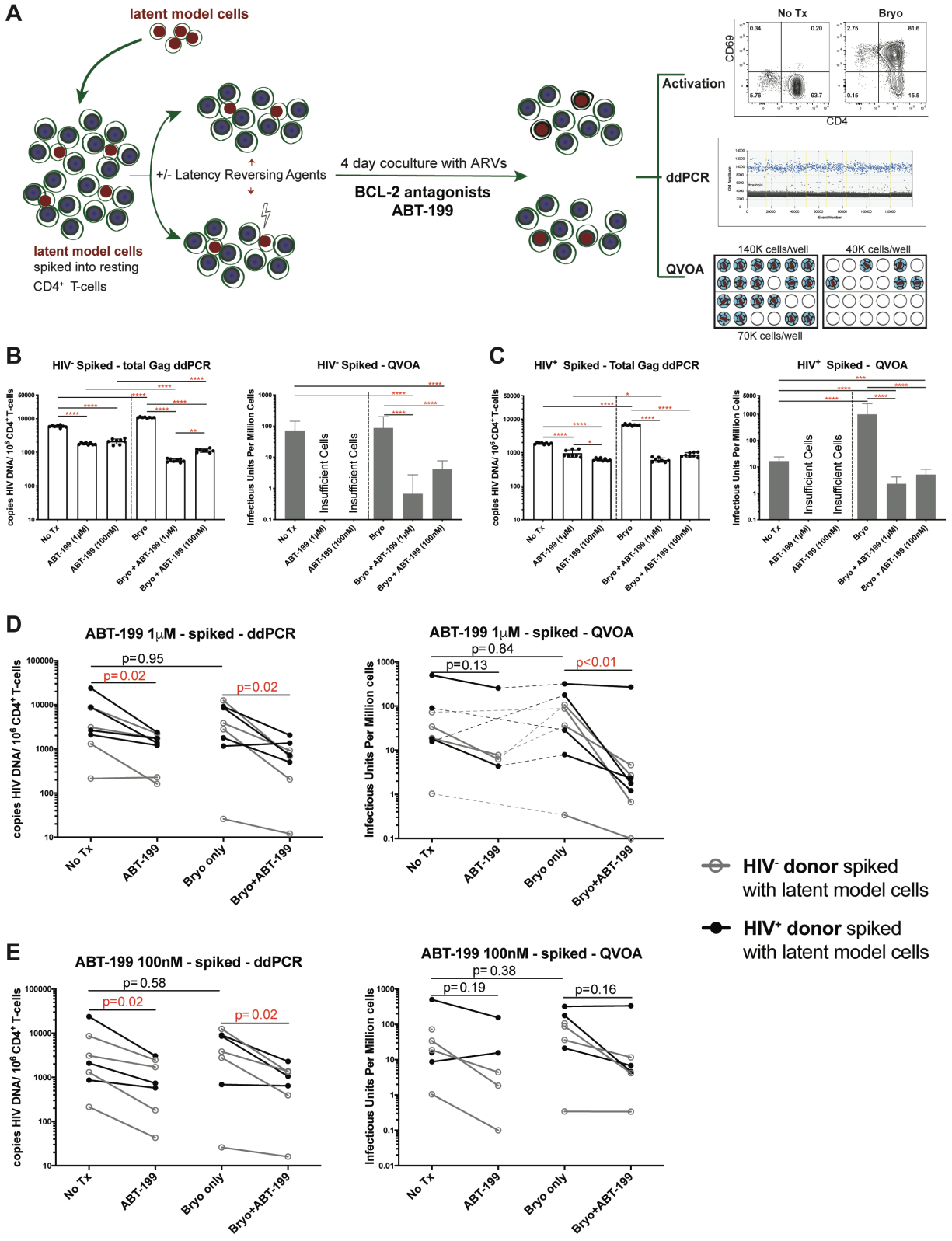

Fig. S5. BCL-2 antagonist drives reductions in total HIV DNA and infectious reservoirs in a primary cell model of latency in "spiked" HIVE assays. (A) Schematic of a HIVE assay "spiked" with a primary cell latency model. Representative "spiked" HIVE assay with cells from an **(B)** HIV-uninfected donor or **(C)** an HIV-infected donor. **Left:** ddPCR results showing the mean ± SD of 8 technical replicates for HIV DNA measured with HIV *gag* primer/ probe set;

right: QVOA results showing IUPM ± 95% confidence interval. Statistical significance determined by: One-way ANOVA for ddPCR, and a Pairwise Chi-Square Test for QVOA (* $p<0.05$, ** $p<0.01$, *** $p<0.001$, **** $p<0.0001$). Summary data showing the effect of **(D)** ABT-199 (1μM) or **(E)** ABT-199 (100nM) on HIV reservoirs from a primary cell latency model. **(D)** Levels of HIV DNA (left) and IUPM (right), comparing treatment with ABT-199 (1μM) vs No Tx, and Bryostatin-1+ABT-199 (1μM) vs Bryostatin-1 (n=8). Dashed lines indicate conditions from a single HIVE assay. **(E)** Comparing treatment with ABT-199 (100nM) vs No Tx, and Bryostatin-1+ABT-199 (100nM) vs Bryostatin-1 (n=7). DMSO was added to NoTx conditions at a matched concentration with +Tx conditions. Statistical significance was determined by Wilcoxon matched-pairs signed rank test.

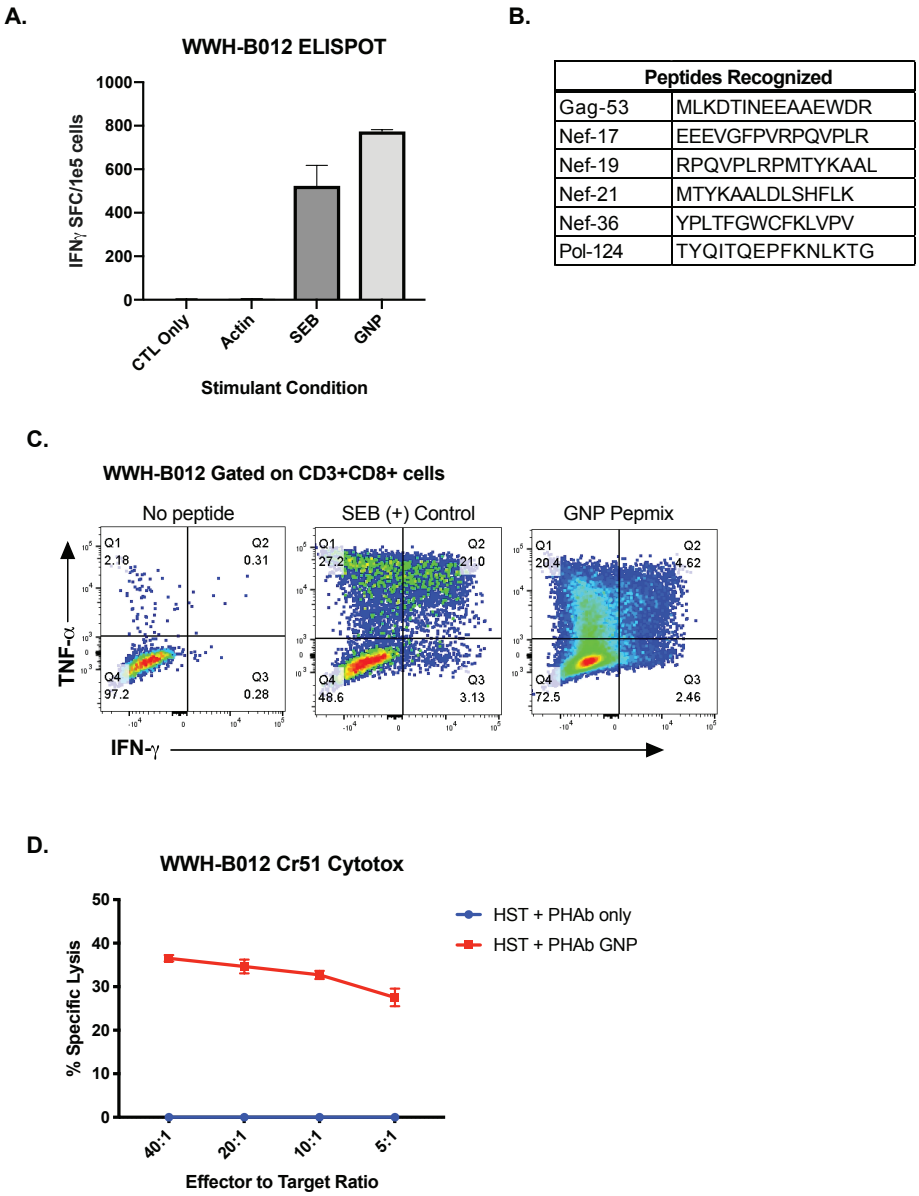

Fig. S6. HIV-specific T-cells (HSTs) are specifically reactive against multiple HIV epitopes, highly cytotoxic, and display a polyfunctional cytokine response. Representative Donor WWH-B012. (A) WWH-B012 HSTs show significant IFN-γ secretion against HIV pepmix by ELISPOT. **(B)** HSTs recognize multiple Gag, Nef, and Pol peptides, as determined by IFN-γ ELISPOT. **(C)** HSTs secrete TNF-α and IFN-γ by intracellular cytokine staining, in response to HIV pepmix stimulation. **(D)** HSTs display lysis of autologous HIV peptide-pulsed PHA blasts at various effector-to-target ratios in a chromium release assay.

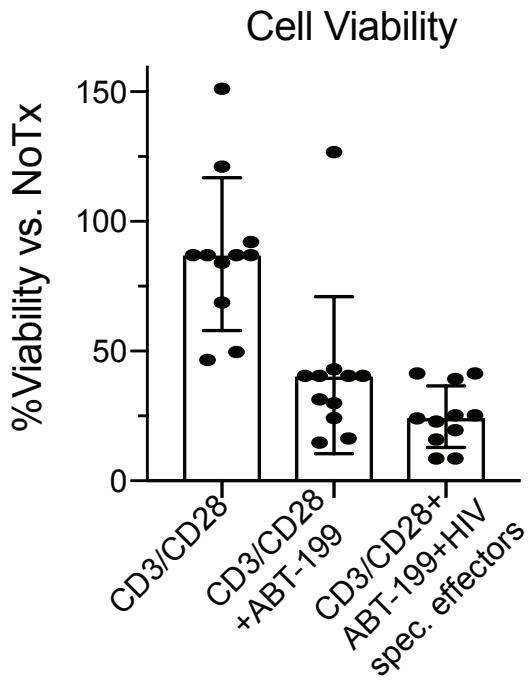

Fig. S7. Cell toxicity of the BCL-2 antagonist ABT-199 on *ex vivo* CD4$^+$ T-cells in HIVE assays. **A)** Viability of CD4$^+$ T-cells at the end of HIVE assays in conditions where they were co-cultured with ABT-199. Viable cells were counted by flow cytometry, in relation to counting beads, and normalized to the viability seen in the NoTx condition. Shown are the means of 10 HIVE assays ± SD.

Supplementary References

1. A. Bosque, V. Planelles, Induction of HIV-1 latency and reactivation in primary memory CD4+ T cells. *Blood* **113**, 58-65 (2009).
2. S. H. Huang *et al.*, Latent HIV reservoirs exhibit inherent resistance to elimination by CD8+ T cells. *J Clin Invest* **128**, 876-889 (2018).
3. S. Lam *et al.*, Broadly-specific cytotoxic T cells targeting multiple HIV antigens are expanded from HIV+ patients: implications for immunotherapy. *Mol Ther* **23**, 387-395 (2015).
4. S. Patel *et al.*, Functionally Active HIV-Specific T Cells that Target Gag and Nef Can Be Expanded from Virus-Naive Donors and Target a Range of Viral Epitopes: Implications for a Cure Strategy after Allogeneic Hematopoietic Stem Cell Transplantation. *Biol Blood Marrow Transplant* **22**, 536-541 (2016).
5. L. J. Martins *et al.*, Modeling HIV-1 Latency in Primary T Cells Using a Replication-Competent Virus. *AIDS Res Hum Retroviruses* **32**, 187-193 (2016).